Electric Power Systems Research 152 (2017) 485–492

Contents lists available at ScienceDirect

Electric Power Systems Research

journal homepage: www.elsevier.com/locate/epsr

Electric field at sharp edge as a criterion for dimensioning condenser-type insulation systems

Dalibor Filipović-Grčić [a], Božidar Filipović-Grčić [b,*], Miroslav Poljak [c]

[a] Končar — Electrical Engineering Institute, Fallerovo šetalište 22, 10000 Zagreb, Croatia
[b] University of Zagreb, Faculty of Electrical Engineering and Computing, Department of Energy and Power Systems, Unska 3, 10000 Zagreb, Croatia
[c] Končar — Electrical Industry Inc., Fallerovo šetalište 22, 10000 Zagreb, Croatia

ARTICLE INFO

Article history:
Received 14 January 2017
Received in revised form 3 August 2017
Accepted 6 August 2017

Keywords:
Oil-paper condenser-type insulation
Electric field
Dielectric stresses
Power transformer bushing
Instrument transformers
Partial discharges

ABSTRACT

Inside the oil-paper insulation of high voltage condenser-type bushings and instrument transformers, conducting surfaces or capacitive shields have been in use for many years to control electric field distribution. Traditional insulation design methods take into consideration dielectric stresses in axial and radial directions, but experience shows that partial discharges occur in the vicinity of capacitive shield edges and can severely affect the expected life of oil-paper insulation. In this paper, a criterion for dimensioning condenser-type insulation systems is presented, based on maximum electric field at sharp edge of capacitive shield. Maximum permitted value of the electric field at the shield's edge was obtained through numerous experimental tests and numerical field calculations based on the finite element method (FEM).

1. Introduction

The most frequent sources of power transformer failures are attributed to tap changers, bushings, and oil-paper insulation system which deteriorates mainly due to heat, oxidation, acidity, and moisture. Bushings are one of the major components causing forced outages of power transformers [1,2]. According to analyses in which individual transformer components are ranked with respect to the number of transformer failures they cause, bushings are placed at one of the top positions [3]. This clearly shows that there is a need for improvement of the existing criteria for the dimensioning of insulation systems, especially in condenser-type transformer bushings.

Modern high-voltage bushings with oil-paper insulation for system voltages higher than 52 kV are condenser-type. The condenser core of a bushing is built up around a central tube that may or may not be in the current-carrying path. It is wound from paper and impregnated with transformer oil. Capacitive shields within oil-paper insulation take the form of coaxial cylinders and constitute a system of cylindrical capacitors, arranged in such a way that the electric stress in both radial and axial directions does not exceed certain critical values. The capacitance between any adjacent pair of capacitive shields is known as a partial capacitance and the bushing insulation is made up of a large number of partial condensers in series. An optimal number of shields and each shield's dimensions lead to acceptable dielectric stresses and the most economical design of insulation system [4,5].

In the traditional design, the maximum axial and radial electric fields in the condenser body should not exceed certain permitted values [6–9]. This approach does not take into account the maximum value of electric field at the shield's edge. However, a real operation experience and laboratory tests indicate that damage caused by partial discharges frequently occurs at the edges of capacitive shields [10–13]. Although the amplitudes of such partial discharges are initially low, their occurrence causes deterioration of insulation properties, premature aging and finally insulation breakdown. The reason why electric field at the shield's edge was not taken into account, as a criterion for sizing the insulation system, lies in the fact that it is very difficult to calculate it accurately, even with the latest software tools, due to unfavourable ratios between minimum and maximum dimensions of the simulation model [14]. The ratio of model height to shield thickness can be several orders of magnitude. For such a model, it is very difficult to obtain the fine mesh density of finite elements what improves calculation accuracy.

* Corresponding author.
E-mail addresses: dfilipovic@koncar-institut.hr (D. Filipović-Grčić), bozidar.filipovic-grcic@fer.hr, bozofilipovic@gmail.com (B. Filipović-Grčić), poljak.dd@koncar.hr (M. Poljak).

http://dx.doi.org/10.1016/j.epsr.2017.08.006
0378-7796/

This paper presents a criterion for dimensioning condenser-type insulation systems. The proposed criterion is based on a method developed for more accurate calculation of electric field at shield's edge. The maximum electric field at the shield's edge should not exceed the partial discharge inception stress, which was determined through numerous laboratory tests on samples that represent bushing insulation [15].

2. Radial and axial electric fields as criteria for dimensioning condenser-type insulation

In traditional approach, capacitive shields within oil-paper insulation are arranged in such a way that the electric stress in the radial direction does not exceed a certain permitted value E_r (typically 13 kV/mm) and so that the axial stress does not exceed a value E_{aa} (typically 0.5 kV/mm) for the air side, and E_{ao} (typically 1.3 kV/mm) for the oil side of the bushing [6]. Axial stress is given as the voltage between adjacent shields divided by the axial distance between the ends of the shields. Condenser bushing details are shown in Fig. 1.

The central tube on which the condenser body is wound is at 100% of the potential, while the last outer shield is grounded. Fig. 1 shows shields numbered from 1 to n, their lengths l, and radiuses r at which they are inserted in the insulation. a represents the axial spacing between the shields from the air side of the bushing while c represents the axial spacing between the shields from the oil side.

The number of shields, and thus of partial condensers, is chosen in such a way that the test voltage of each condenser does not exceed a specific value. All things considered, the task is to determine the physical dimensions of shields which give the most economical design. Essentially, the design of bushings may be based upon several methods, but the most favourable design is obtained by considering equal partial capacitances and equal axial steps between shields, separately for air and oil sides. This method gives a linear voltage distribution in the axial direction and this is important since dielectric strength in the axial direction is significantly less than strength in the radial direction.

As the axial spacing between shields at both air and oil sides are constant, with a linear distribution of potential, axial stresses at the air and the oil side are uniform. However, the distribution of radial electric field is not linear and has a saddle shape with equal maximum radial field between the central tube and the first shield, and also between the second last and the last shield, while radial field between the other shields are lower. A typical distribution of the radial field E_r and axial field E_{ao} at the oil side is shown in Fig. 2 [15].

Axial distance a between the ends of adjacent shields on the air side of the bushing is determined as:

$$a = \frac{U}{n \cdot E_{aa}}, \tag{1}$$

where U represents the applied voltage and n the number of shields. Similarly, the axial distance c between the ends of adjacent shields on the oil side of the bushing is determined as:

$$c = \frac{U}{n \cdot E_{ao}}. \tag{2}$$

Maximum radial field between shields $i-1$ and i is determined from the expression:

$$E_{ri} = \frac{U_i}{r_{i-1} \ln \frac{r_i}{r_{i-1}}}, \tag{3}$$

where U_i is the voltage drop between the shields $i-1$ and i. From expression (3) it follows:

$$\frac{U_i}{r_{i-1} E_{ri}} = \ln \frac{r_i}{r_{i-1}}. \tag{4}$$

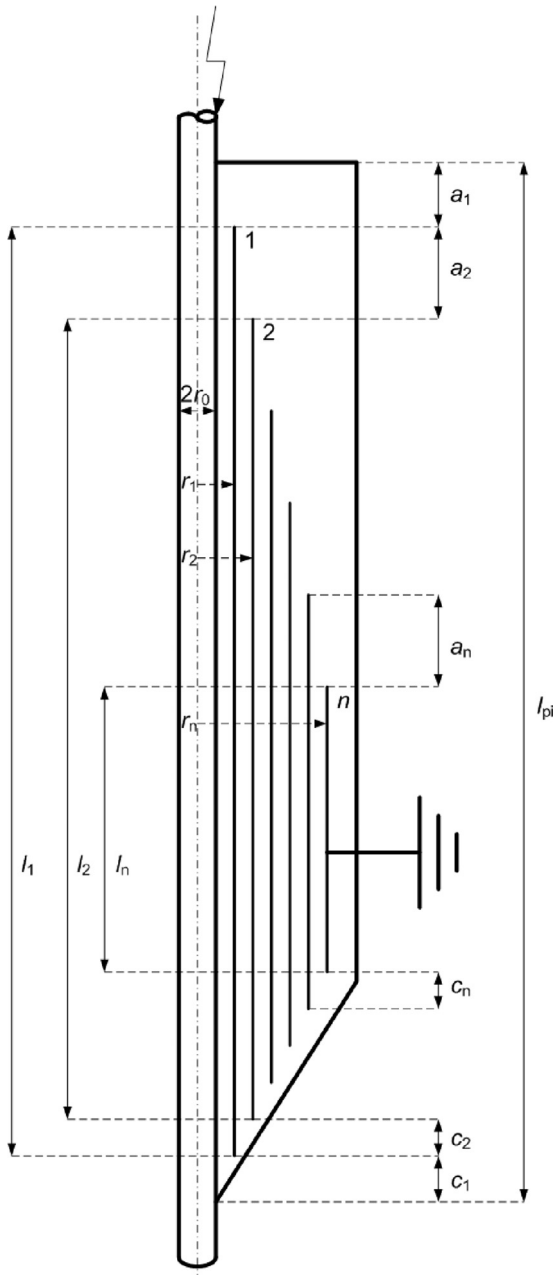

Fig. 1. Condenser bushing details.

Sum of expression (4) for $i = 1 \ldots n-1$ gives:

$$\sum_{i=1}^{n-1} \frac{U_i}{r_{i-1} E_{ri}} = \sum_{i=1}^{n-1} \ln \frac{r_i}{r_{i-1}} = \ln \frac{r_{n-1}}{r_0}. \tag{5}$$

Expression (5) can be written as:

$$\ln \frac{r_{n-1}}{r_0} - \ln \frac{r_1}{r_0} = \sum_{i=2}^{n-1} \ln \frac{r_i}{r_{i-1}}. \tag{6}$$

Linear distribution of potential across the shields is obtained if the capacitances between the shields are equal:

$$\frac{2\pi\varepsilon l_1}{\ln \frac{r_1}{r_0}} = \frac{2\pi\varepsilon l_2}{\ln \frac{r_2}{r_1}} = \ldots = \frac{2\pi\varepsilon l_n}{\ln \frac{r_n}{r_{n-1}}}. \tag{7}$$

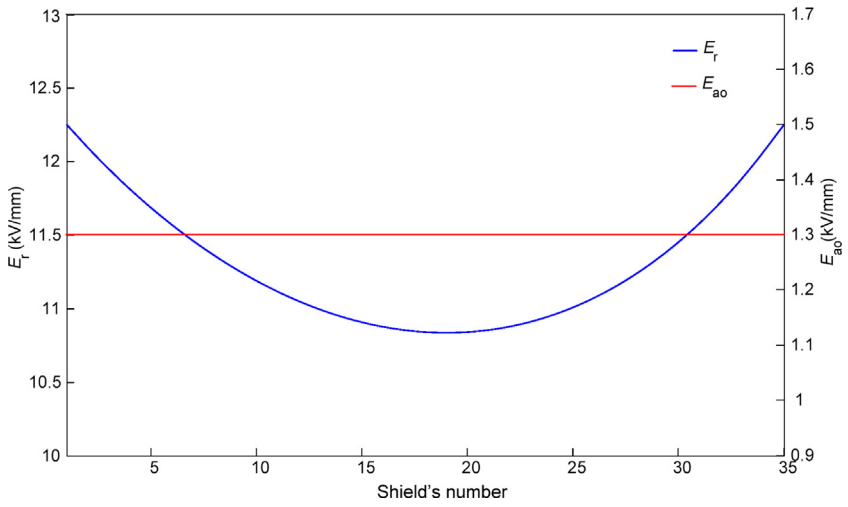

Fig. 2. A typical distribution of the radial and axial electric field at the oil side of the bushing.

From the equality of capacitance between the first shield and the central tube to all other capacitances it follows:

$$\ln\frac{r_i}{r_{i-1}} = \frac{l_i}{l_1}\ln\frac{r_1}{r_0}. \tag{8}$$

Substituting Eq. (7) with Eq. (8) gives:

$$\ln\frac{r_{n-1}}{r_0} - \ln\frac{r_1}{r_0} = \left(\sum_{i=2}^{n-1}\frac{l_i}{l_1}\right)\ln\frac{r_1}{r_0}. \tag{9}$$

Expression (9) can be written as:

$$\ln\frac{r_{n-1}}{r_0} = \ln\frac{r_1}{r_0}\sum_{i=1}^{n-1}\frac{l_i}{l_1}. \tag{10}$$

In the case of uniform distribution of axial fields, radial distribution, as mentioned above, may not be linear, but has a saddle shape. In this case, the most favourable situation is if the values of the radial field for the first and the last capacitor are equal:

$$\frac{U_1}{r_0\ln\frac{r_1}{r_0}} = \frac{U_n}{r_{n-1}\ln\frac{r_n}{r_{n-1}}}. \tag{11}$$

As the potential distribution is linear or voltages across capacitors are equal, from the expression (11) it follows:

$$\frac{r_0}{r_{n-1}} = \frac{\ln\frac{r_n}{r_{n-1}}}{\ln\frac{r_1}{r_0}}. \tag{12}$$

If the right side of Eq. (12) is substituted with Eq. (8) for $i = n$ then the following expression is obtained:

$$\frac{r_0}{r_{n-1}} = \frac{l_n}{l_1} = \alpha, \tag{13}$$

where the parameter α represents the ratio of the length of the last and the first shield. From the expressions (9) and (13) it follows:

$$\ln\frac{r_1}{r_0}\sum_{i=1}^{n-1}\frac{l_i}{l_1} = \ln\frac{1}{\alpha}. \tag{14}$$

A parameter λ is introduced that depends on the applied voltage U, the diameter of the central tube r_0 and a given radial field E_r:

$$\lambda = \frac{U}{2r_0E_r}. \tag{15}$$

Since the radial field is highest in the first and the last capacitor, from Eqs. (15) and (3) it follows:

$$\ln\frac{r_1}{r_0} = \frac{2\lambda}{n}. \tag{16}$$

Inserting expression (16) into (14) gives:

$$-\frac{2\lambda}{nl_1}\sum_{i=1}^{n-1}l_i = \ln\alpha. \tag{17}$$

The length of the last shield l_n can be expressed by the length of the first shield l_1, the number of shields n and the sum of axial distances from the air side a, and the oil side c:

$$l_n = l_1 - (n-1)(a+c). \tag{18}$$

From Eq. (18), for $a + c = \Delta$, it follows:

$$\Delta = \frac{l_1 - l_n}{n-1}. \tag{19}$$

The sum of the lengths of all shields except the last one may be expressed by the length of the first shield, the sum of axial distances and the number of shields:

$$\sum_{i=1}^{n-1}l_i = l_1 + (l_1 - \Delta) + (l_1 - 2\Delta) + \ldots + (l_1 - (n-2)\Delta) \tag{20}$$

$$\sum_{i=1}^{n-1}l_i = (n-1)l_1 - \Delta(1 + 2 + \ldots + (n-2)) \tag{21}$$

$$\sum_{i=1}^{n-1}l_i = (n-1)l_1 - \Delta\frac{(n-2)(n-1)}{2} \tag{22}$$

$$\sum_{i=1}^{n-1}l_i = (n-1)\frac{2l_1 - (n-2)\Delta}{2}. \tag{23}$$

Inserting expression (19) into (23) gives:

$$\sum_{i=1}^{n-1}l_i = \frac{nl_1 + (n-2)l_n}{2}. \tag{24}$$

Inserting expression (24) into (17) gives:

$$\lambda = -\frac{n\ln\alpha}{(n-2)\alpha + n}. \tag{25}$$

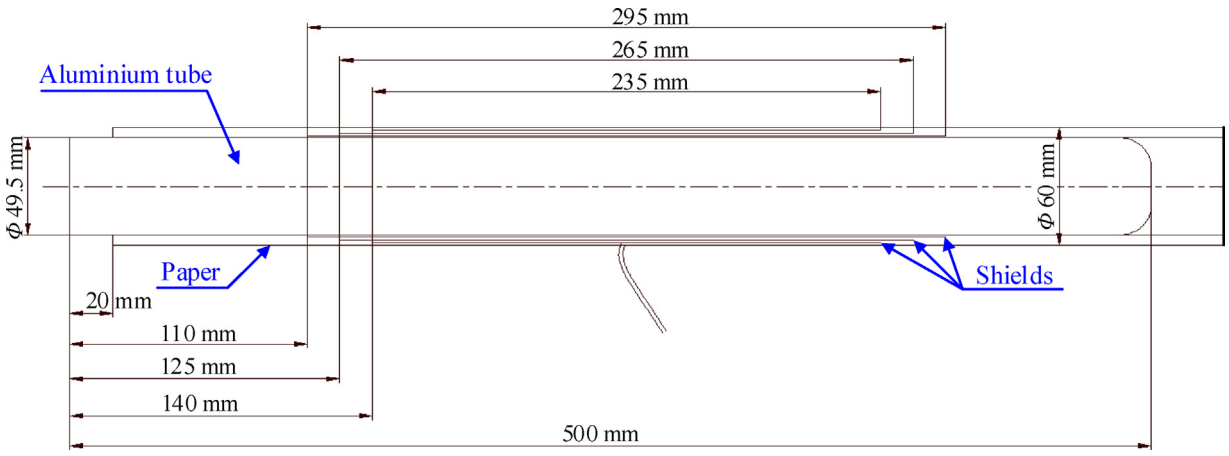

Fig. 3. Sample of insulation.

In the expression (25) the only unknown parameter α represents the ratio of the lengths of the last and the first shield. This equation has no analytical solution and it can be solved only numerically. Once parameter α is determined, the length of the first shield can be obtained from Eq. (19), for $l_n = \alpha l_1$:

$$l_1 = \Delta \frac{n-1}{1-\alpha}. \tag{26}$$

Afterwards, the lengths of all other shields can be determined from:

$$l_i = l_1 - (i-1)\,\Delta\,. \tag{27}$$

Finally, when the lengths of all shields are determined, their radiuses, starting from the first, are calculated from the following recursive expression that is obtained after inserting expression (16) into (8):

$$r_i = r_{i-1} e^{\frac{2\lambda l_i}{n l_1}}\,. \tag{28}$$

So, for the given input parameters from the expressions (1), (2) and (15) axial distances from the air and oil sides are determined. Afterwards, the numerical solution α of Eq. (25) is obtained, which gives the ratio of the lengths of the last and the first shield. With the known parameters of the Eqs. (26)–(28), the lengths and radiuses of all shields are determined that provide an ideal voltage distribution.

3. Experimental testing of insulation model

3.1. Test setup

The model that represents the condenser-type insulation consists of three capacitive shields placed inside oil-paper insulation that is wound around an aluminium tube with diameter 49.5 mm (Fig. 3). The thickness of the insulation between shields and axial spacing correspond to those used in real bushings, and the thickness of the shield is 20 μm.

Three samples were dried along with real bushings in the production. They were subjected to standard vacuum drying with hot air for 7 days followed by impregnation with dried and degassed oil. A settling time of 7 days was provided before the commencement of HV tests.

The test voltage levels were chosen to cause levels with low, medium and high probabilities of partial discharges. Voltage was applied on the central tube and the outermost shield was earthed. The voltage on each sample was maintained until partial discharge inception occurred or up to one hour in the event of no discharges. If the partial discharges occurred at a certain voltage, the next test value was one level lower or, in case of no occurrence, one level higher. This test procedure is classified as non-destructive and, when the sample is given a suitable rest time after the test, it can be considered that insulation properties return to the initial condition [16]. In this way, many tests can be repeated on the same sample.

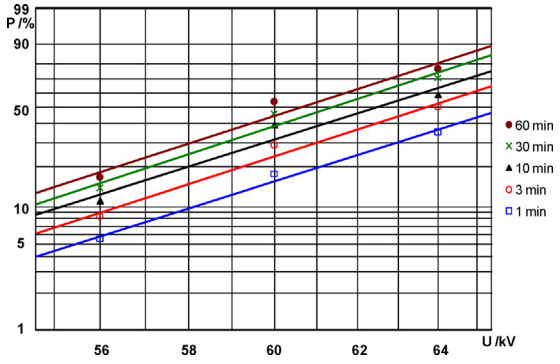

Fig. 4. Weibull curves showing probability of partial discharge inception.

3.2. Test results

For each voltage level, test results (given in Table 1) consist of a series of values of the time elapsed until partial discharge inception. These values are grouped into five time intervals. The number of partial discharge inceptions N_i for each interval expressed as a percentage of the total number of tests N at that voltage level gives the probability P of partial discharge inception in percentage terms.

$$P = f(U)\,\mathrm{t} = \mathrm{const.} \tag{29}$$

The results in Table 1 can be presented in the form of a family of curves. Partial discharge inception probability can be accurately represented using the Weibull distribution with a lower limit equal to zero:

$$P = 1 - e^{(-AU^{\alpha}t^{\beta})}, \tag{30}$$

where A, α and β are constants. The experimental results of Table 1 are plotted on a special chart having the P scale proportional to $\ln(\ln(1/(1-P)))$, and the U scale proportional to $\ln(U)$. Using the method of least squares a family of almost parallel straight lines is defined as shown in Fig. 4. The insulation system with very low probability of partial discharge inception during a 1 min power-frequency voltage withstand test can be considered as highly reliable. If the straight line for time interval $t < 1$ min is extrapolated, then the probability of partial discharge inception value of 1% corresponds to a voltage value of 49.9 kV.

Table 1
Results obtained on samples.

U (kV)	N	$t<1$ min		$t<5$ min		$t<10$ min		$t<30$ min		$t<60$ min	
		N_i	P (%)	N_i	P (%)	N_i	P (%)	N_i	P (%)	N_i	P (%)
56	36	2	5.56	3	8.33	4	11.11	5	13.89	6	16.67
60	56	10	17.86	16	28.57	22	39.29	26	46.43	30	53.57
64	34	12	35.29	17	50	20	58.82	24	70.59	26	76.47

Table 2
Breakdown voltage values.

Sample no.	1	2	3
Type of breakdown voltage	LI	SI	AC
U (kV)	201.2	171.6	77.0

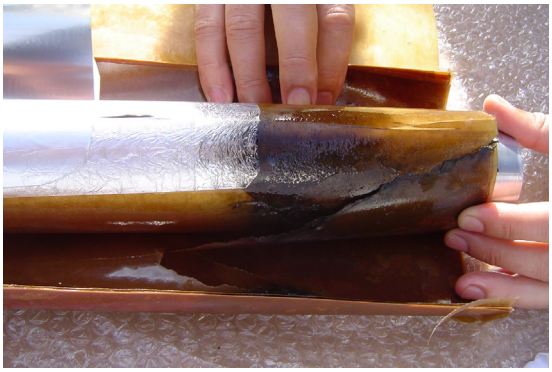

Fig. 5. Sample no. 2 — insulation breakdown pathway.

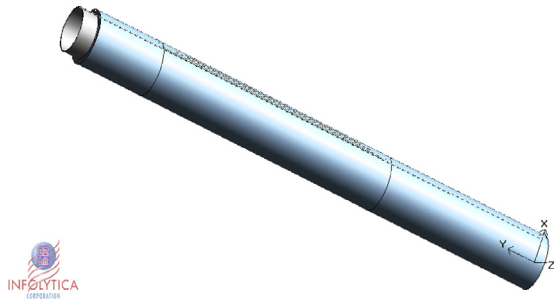

Fig. 6. Model of insulation for numerical calculation.

Finally, each sample was subjected to various kinds of increasing dielectric stress until breakdown occurred. The first sample was subjected to a lightning impulse voltage (LI), the second to a switching impulse voltage (SI), and the third to AC voltage. The breakdown voltage values are given in Table 2.

Fig. 5 shows insulation breakdown pathway in sample no. 2.

It was found that in all three samples a critical place where a breakdown occurs is from the shield's edge towards the central tube. This proves the fact that designing process of the insulation system should take into account the maximum electric field value on the shield's edge, which is discussed in the following chapter.

4. Method for calculation of electric field at shield's edge

The numerical calculation has been performed using the FEM-based software ElecNet. Owing to the axial symmetry present in this part of the insulation system, ElecNet's 2D Axially Symmetric Static solver was used. The calculation model, with relative permittivity of oil 2.2 and relative permittivity of oil-impregnated paper 3.6, is shown in Fig. 6 and it corresponds to experimental samples (Fig. 3).

A voltage was applied on the central tube while two inner shields are represented as floating electrodes at free potential. The peak value of electric field occurs at the place with the highest potential gradient. That place is the edge of the last (outer) shield which is grounded. Since the shields are very thin, their thickness compared to the largest model dimension yields an order of four. Therefore, a different approach for calculation of electric field on shield's edge was applied that consists of two steps.

In the first step, a large-scale model with sufficiently fine mesh is used to determine the potential distribution near the shield's edge (Fig. 7).

An equipotential line near the shield's edge is selected to represent one of the boundaries of a fine scaled model for calculation of electric field at the shield's edge (Fig. 8). Post-processing software analyses large scale model field and extracts points that lie on the equipotential line with tolerance ±1%. Other boundaries are electric field lines. Software extracts points that lie on electric field lines by moving in the direction of highest field.

In the second step, a fine scaled model is formed which contains the shield's edge and the surrounding insulation. In this model, it is possible to obtain a fine mesh of finite elements and thus to calculate electric field at shield's edge with sufficient accuracy.

The result of numerical calculation for the model shown in Fig. 6 is shown in Fig. 9. The maximum value of electric field 0.25 kV/mm was obtained at the last shield's edge which is grounded when 0.1 kV was applied on the central tube. The value of the electric field for any other value of the applied voltage U (kV) can be determined as:

$$E_s = 0.25\frac{U}{0.1}(\text{kV/mm}). \tag{31}$$

When related to experimental test results, the value of the electric field on the shield's edge with a low probability of partial discharge occurrence for certain time intervals can be calculated. For example, when the applied voltage is 49.9 kV ($t<1$ min, $P=1\%$) the observed electric field value reaches almost 125 kV/mm and is established as a criterion for dielectric field stress at the shield's edge. It should be noted that field values at the edge of the shields should be lower than the proposed 125 kV/mm. The reason for this is that the physical mechanism of partial discharges is not sufficiently known and may change with time and shield arrangement. Also, the mathematical model used may not be valid for extended time ranges and the effect of temperature and moisture on partial discharge occurrence was not investigated. Furthermore, stressed insulation volume in considered models is smaller than the one in actual insulation systems. Therefore, a safety margin must be taken into consideration and the permissible electric field should be lower than 100 kV/mm.

5. New analytical expression for calculation of electric field at shield's edge

In the previous section the procedure for calculating electric field on the edge of the shield was described. However, inside the condenser-type bushing there are many shields and it would be very time consuming to perform that procedure on each of them. Therefore, an analytical expression for electric field at the shield's

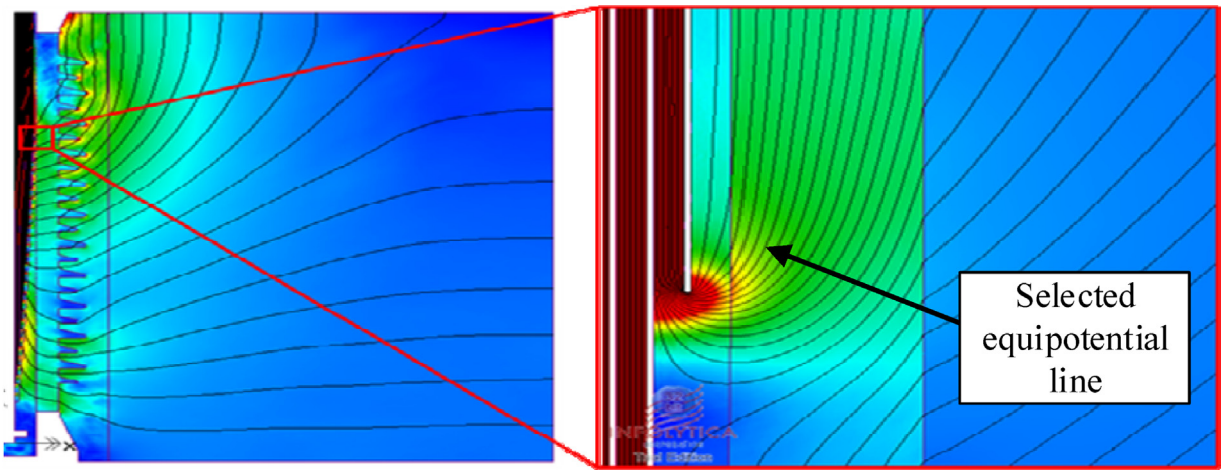

Fig. 7. Method for calculation of electric field strength at the edge of shield — selection of equipotential line.

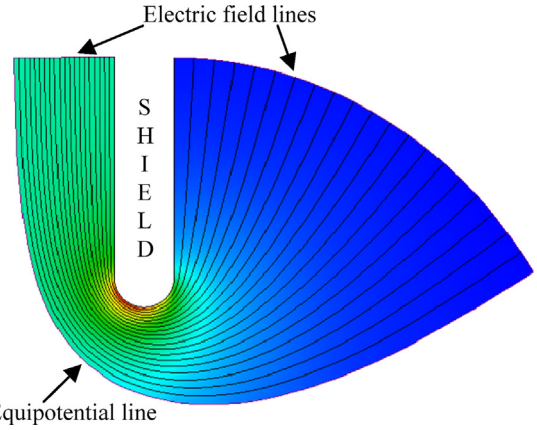

Fig. 8. Selected borders of a new scaled model for calculation of electric field strength around shield's edge.

edge was derived. Numerical field calculations were performed in order to obtain the relationship between electric field value at the edge of the shield and the thickness of insulation between two adjacent shields, axial distance between edges of two adjacent shields and the thickness of the shield itself.

At first, the influence of insulation thickness d (radial distance) between two adjacent shields and thickness d_s of the shield itself were analysed on a model shown in Fig. 10. The model consists of a metal tube with a radius r_0 to which a voltage is applied and a grounded shield with a radius r_1.

Four different thicknesses of the shield (20, 50, 100 and 140 μm) were considered as well as ten different thicknesses of insulation. The influence of insulation thickness and shield's thickness on the electric field value at the edge of the shield is shown in Fig. 11.

After the fitting of results, it is shown that these two parameters affect the field value according to the following expression:

$$E_S = K_1 d^{-k_2}\,. \tag{32}$$

K_1 is a parameter proportional to the voltage between two adjacent shields and it decreases as the thickness of the shield is increased:

$$K_1 = 0.12 d_s^{-0.47}. \tag{33}$$

K_2 is a parameter which increases linearly with the thickness of the shield:

$$K_2 = 0.49 d_s + 0.51\,. \tag{34}$$

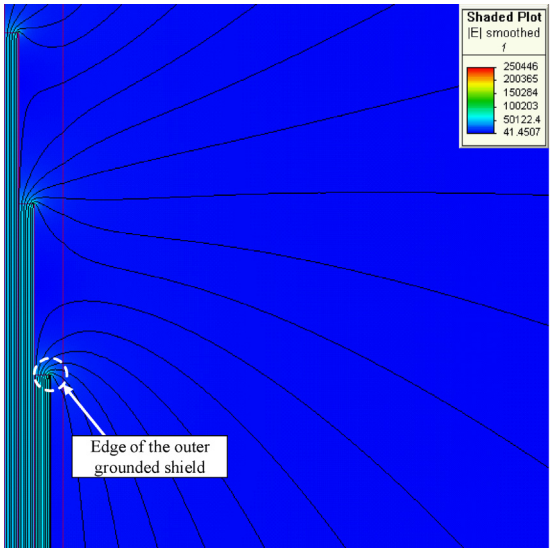

Fig. 9. Distribution of electric field strength and equipotential lines.

Expression (32) can now be used to obtain the electric field value at the shield's edge.

The influence of axial distance a between the edges of two adjacent shields on the electric field value at the edge of the shield, while all other dimensions remained constant, was analysed using the model shown in Fig. 12 which consists of two shields.

A voltage was applied on the inner shield with a radius r_1, while the outer shield with a radius r_2 was grounded. Electric field was calculated at the edge of the grounded shield. The results showed that in actual design the influence of axial distance between the edges of two adjacent shields on the electric field value at the edge of the shield can be neglected. This statement is valid only when axial distances are significantly larger than radial distances, which is normally the case in practice.

6. Application of a new criterion for dimensioning of condenser-type insulation system

A new criterion for dimensioning condenser-type insulation systems, which is based on maximum electric field at sharp edge of capacitive shield, was applied in the case of transformer bushing with highest voltage for equipment U_m = 245 kV. Typically, the number of shields is obtained by dividing the AC withstand voltage

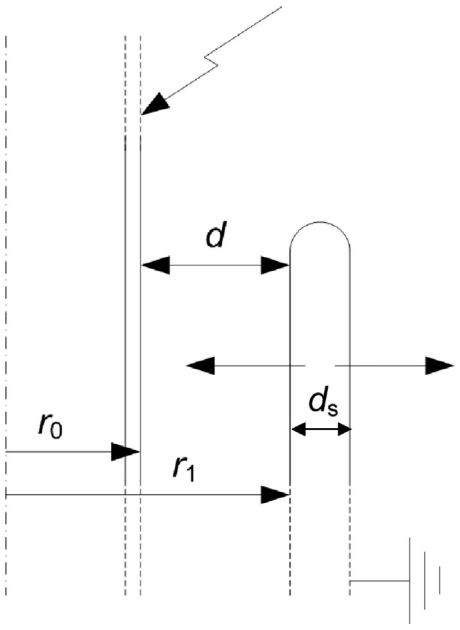

Fig. 10. Model for determining the influence of insulation and shield's thickness on the electric field value at the edge of the shield.

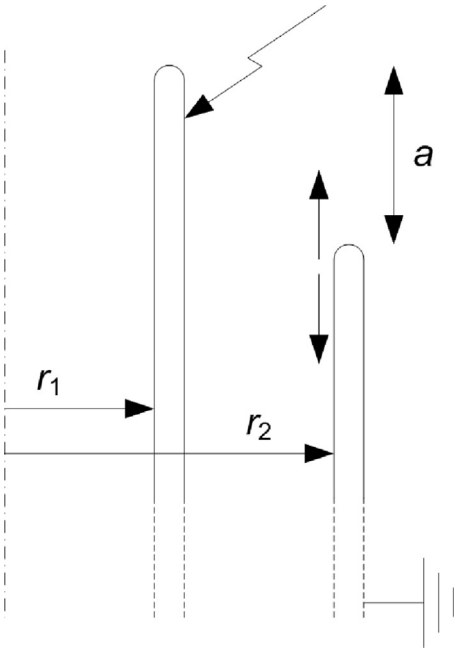

Fig. 12. Model for determining the influence of axial distance between edges of two adjacent shields on the electric field value at the edge of the shield.

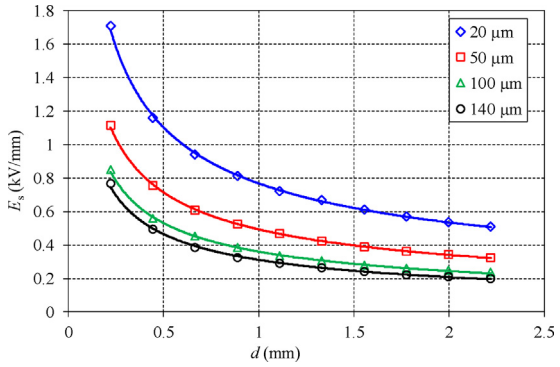

Fig. 11. Influence of insulation thickness and shield's thickness on the electric field value at the edge of the shield for a voltage of 100 V (the lines are fitted according to expression (32)).

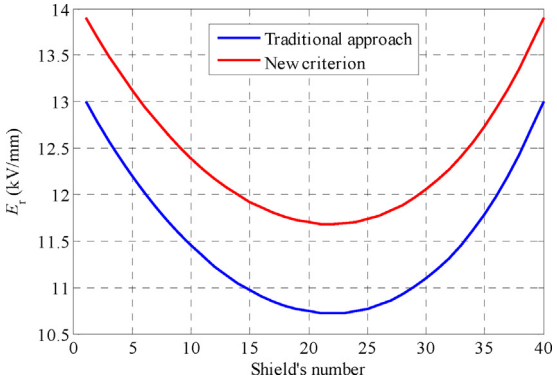

Fig. 13. Electric field in the radial direction as a function of shield's number.

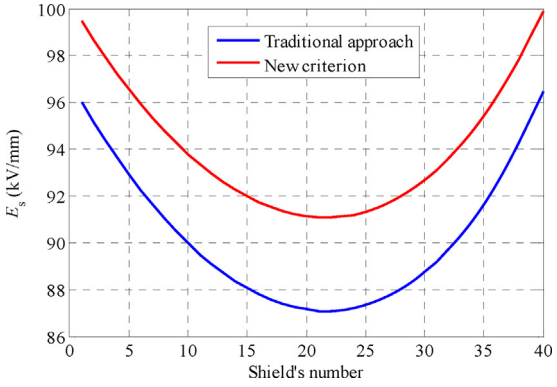

Fig. 14. Electric field at the shield's edge as a function of shield's number.

in kV with number between 10 and 15, meaning that one shield is added for each 10–15 kV of AC withstand voltage. AC withstand voltage for transformer bushing with U_m = 245 kV is 506 kV, so the selected number of shields is 40.

First, traditional approach was used where capacitive shields within oil-paper insulation were arranged in such a way that the electric stress in radial direction did not exceed 13 kV/mm and axial stress did not exceed a value 0.5 kV/mm for the air side, and 1.3 kV/mm for the oil side of the bushing. After that, electric field at the shields edges was calculated with Eq. (32). Calculated electric field in the radial direction E_r and electric field at the shield's edge E_s as a function of shield's number are shown in Figs. 13 and 14.

In traditional approach, maximum value of E_r does not exceed 13 kV/mm, while maximum value of E_s is 96.5 kV/mm. This value is lower than the proposed critical value of 100 kV/mm. By applying a new criterion, maximum value of E_s is limited to 100 kV/mm, what caused E_r to rise above 13 kV/mm and reach 13.9 kV/mm.

Fig. 15 shows geometrical arrangement of shields within the insulation system obtained by traditional approach and the new criterion. As can be seen from Fig. 15, the dimensions of the insulation system were reduced when a new criterion was applied. In

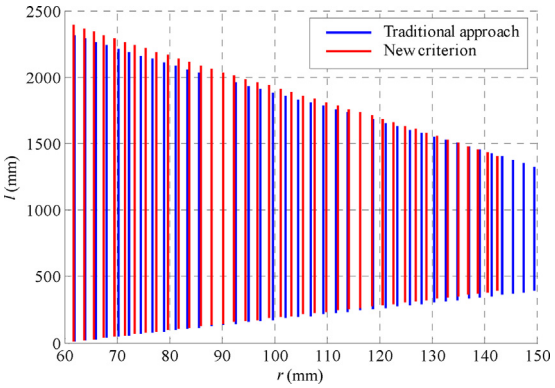

Fig. 15. Geometrical arrangement of shields within the insulation system obtained by traditional approach and the new criterion.

the particular case, the volume of paper insulation was reduced by 7.3%.

7. Conclusion

A new criterion for dimensioning of condenser-type insulation systems is presented which is based on maximum electric field strength at sharp edge of capacitive shield. The maximum electric field strength at the shield's edge should not exceed the partial discharge inception stress, which was determined through numerous laboratory tests on samples that represent bushing insulation. A method for more accurate calculation of electric field at shield's edge is proposed based on finite element method.

Since an insulation system of the condenser-type bushing contains many shields, it would be very time consuming to perform calculations of electric field at shield's edge based on finite element method. Therefore, an analytical expression for calculation of electric field at the shield's edge was derived which has been applied in the development of insulation system for HV transformer bushings with highest voltage U_m = 245 kV. The volume of the transformer bushing insulation system obtained with the new criterion, which is based on maximum electric field at sharp edge of capacitive shield, was reduced by 7.3% compared to traditional approach, which is based on electric fields in the radial and axial direction. The bushing successfully passed all routine and type tests in accordance with Ref. [17].

References

[1] S.M. Gubanski, P. Boss, G. Csépes, V. Der Houhanessian, J. Filippini, P. Guuinic, U. Gäfvert, V. Karius, J. Lapworth, G. Urbani, P. Werelius, W. Zaengl, "Dielectric Response Methods for Diagnostics of Power Transformers", CIGRE Technical Brochure no. 254 — Report of the Task Force D1.01.09, Paris, 2002.
[2] N. Hashemnia, A. Abu-Siada, S. Islam, Detection of power transformer bushing faults and oil degradation using frequency response analysis, IEEE Trans. Dielectr. Electr. Insul. 23 (February (1)) (2016) 222–229.
[3] A. Mikulecky, Z. Stih, Influence of temperature, moisture content and ageing on oil impregnated paper bushings insulation, IEEE Trans. Dielectr. Electr. Insul. 20 (August (4)) (2013) 1421–1427.
[4] E. Kuffel, W.S. Zaengl, J. Kuffel, High Voltage Engineering Fundamentals, Newnes, Oxford, 2000, pp. 201–394.
[5] V. Bego, Instrument Transformers, Školska knjiga, Zagreb, 1977.
[6] J.A. Güemes, M. Postigo, A. Ibero, Influence of leader shields in the electric field distribution in current transformers, in: 10th Mediterranean Electrotehnical Conference MELECON, vol. III, Nicosia, Cyprus, 2000, pp. 958–961.
[7] J.A. Güemes, M. Postigo, F.E. Hernando, Influence of leader shields in the electric field distribution in bushings, in: Conference Record of the IEEE Industry Applications Conference, vol. I, Rome, Italy, 2000, pp. 698–703.
[8] E. Lesniewska, The use of 3-D electric field analysis and the analytical approach for improvement of a combined instrument transformer insulation system, IEEE Trans. Magn. 38 (March (2)) (2002).
[9] E. Lesniewska, New approach of applying capacitance control in the main insulation of HV instrument transformers, in: International Symposium on Electromagnetic Fields in Mechatronics, Electrical and Electronic Engineering ISEF 2005, Baiona, Spain, September, 2005.
[10] M. Poljak, D. Filipović-Grčić, Optimization of instrument transformer insulating system, in: 7th Croatian CIGRÉ Session, Cavtat, Croatia, 2005.
[11] Z. Fang, J. Jicun, Z. Ziyu, Optimal design of HV transformer bushing, in: Proceedings of the 3rd International Conference on properties and Applications of Dielectric Materials, Tokyo, Japan, 1991, pp. 434–437.
[12] J.V. Champion, S.J. Dodd, Inter-foil electrical breakdown in high voltage ERIP condenser bushing, WG 12.03 of the study committee 12 of the international CIGRE, Electra (December (67)) (1979) 17–28.
[13] M. Pompili, C. Mazzetti, Partial discharge behaviour in switching-surge-aged oil-paper capacitor bushing insulation, IEEE Trans. Dielectr. Electr. Insul. 9 (February (1)) (2002) 104–111.
[14] H. Wang, Z. Peng, S. Zhang, P. Liu, Simulation study of edge effect in high voltage condenser bushing foils, in: IEEE International Conference on Solid Dielectrics (ICSD), Bologna, 2013, pp. 960–962.
[15] D. Filipović-Grčić, Optimization of condenser type insulation system made of oil impregnated paper, in: Doctoral thesis, University of Zagreb, Faculty of Electrical Engineering and Computing, Zagreb, Croatia, 2007.
[16] S. Yakov, Volt–time relationships for PD inception in oil paper insulation, Electra (December (67)) (1979) 17–28.
[17] International Electrotechnical Commission, IEC 60137: Insulated Bushings for Alternating Voltages above 1000 V, International Electrotechnical Commission, 2008, July.

Dalibor Filipović-Grčić was born in Sinj, Croatia, in 1980. He received the Ph.D. degree in electrical engineering and computing from the University of Zagreb, Croatia, in 2010. Currently, he is the Head of the Transformer Department and High-Voltage Laboratory in Končar Electrical Engineering Institute, Zagreb. His areas of interest include high-voltage test and measuring techniques, instrument and power transformers, and insulation systems optimization. Dr. Filipović-Grčić is a member of the technical committees TC E 38 Instrument Transformers and TC E 42 High Voltage Test Techniques.

Božidar Filipović-Grčić was born in Sinj, Croatia, in 1983. He received the B.Sc. and Ph.D. degrees in electrical engineering and computing from the University of Zagreb, Croatia, in 2007 and 2013, respectively. Currently, he is with the Faculty of Electrical Engineering and Computing (Department of Energy and Power Systems), University of Zagreb. He is the Head of Quality in the High-Voltage Laboratory. His areas of interest include power system transients, insulation coordination, and high-voltage engineering. Dr. Filipović-Grčić is a member of the CIGRÉ Study Committees A3 – High Voltage Equipment and C4 – System Technical Performance.

Miroslav Poljak was born in Sinj, Croatia, in 1955. He received his M.Sc. and Ph.D. degrees in electrical engineering from the University of Zagreb, Faculty of Electrical Engineering and Computing in 1988 and 2006, respectively. Since 1978 he has been working in Končar — Group on research and development of instrument transformers. Currently, he is Member of the Managing Board of Končar-Electrical Industry Inc. His research activity is focused on computation and analysis of transient performance of instrument transformers, high-voltage tests, diagnostics of power and instrument transformers. He is Chairman of National technical committees TC E 38 Instrument Transformers and a member of the CIGRÉ Study Committees A3 — High Voltage Equipment.